

# CHANNEL SIMULATION FOR DIRECT DETECTION OPTICAL COMMUNICATION SYSTEMS

M. TYCZ  
M. W. FITZMAURICE

(NASA-TM-X-70562) CHANNEL SIMULATION FOR  
DIRECT DETECTION OPTICAL COMMUNICATION  
SYSTEMS (NASA) 26 p HC \$3.50 CSCL 20E

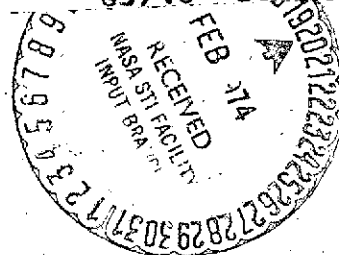
N74-16190

Unclas  
28983

G3/16

**NOVEMBER 1973**

**GODDARD SPACE FLIGHT CENTER**  
**GREENBELT, MARYLAND**



**CHANNEL SIMULATION FOR DIRECT DETECTION  
OPTICAL COMMUNICATION SYSTEMS**

**M. Tycz  
and  
M. W. Fitzmaurice**

**November 1973**

**GODDARD SPACE FLIGHT CENTER  
Greenbelt, Maryland**

CHANNEL SIMULATION FOR DIRECT DETECTION  
OPTICAL COMMUNICATION SYSTEMS

by  
M. Tycz  
and  
M. W. Fitzmaurice

ABSTRACT

A technique is described for simulating the random modulation imposed by atmospheric scintillation and transmitter pointing jitter on a direct detection optical communication system. The system is capable of providing signal fading statistics which obey log normal, beta, Rayleigh, Ricean or chi-squared density functions. Experimental tests of the performance of the Channel Simulator are presented.

**PRECEDING PAGE BLANK NOT FILMED**

## CONTENTS

	<u>Page</u>
ABSTRACT . . . . .	iii
INTRODUCTION . . . . .	1
CHANNEL SIMULATOR SYSTEM CONCEPT . . . . .	2
OPTICAL SUBSYSTEM . . . . .	2
PROCESSING ELECTRONICS . . . . .	6
Atmospheric Log Normal Channel . . . . .	6
Atmospheric Rayleigh and Ricean Channel . . . . .	9
Free Space Channel . . . . .	10
COMPONENT TRANSFER FUNCTION TEST RESULTS . . . . .	10
STATISTICAL FUNCTION TEST RESULTS . . . . .	11
CONCLUSIONS . . . . .	17
ACKNOWLEDGEMENTS . . . . .	20
REFERENCES . . . . .	20

## ILLUSTRATIONS

<u>Figure</u>		<u>Page</u>
1	Direct detection optical communication channels . . . . .	2
2	Channel simulator induced random signal perturbations . . . . .	3
3	Electrooptic modulation – transverse mode . . . . .	4
4	Channel simulator processing electronics a) composite of all channels b) log normal atmospheric channel c) Rayleigh or Ricean atmospheric channel d) beta free space channel. . . . .	7
5	Transfer functions of mathematical operations. . . . .	12

## ILLUSTRATIONS (Continued)

<u>Figure</u>		<u>Page</u>
6	Transfer function of the linearized acoustooptic modulator. . . . .	15
7	Comparison of channel simulator log-normal statistics with GEOS-B data. . . . .	16
8	Statistical test of beta channel . . . . .	18
9	Statistical test of Rayleigh random voltage mode of operation . . . . .	19

# CHANNEL SIMULATION FOR DIRECT DETECTION OPTICAL COMMUNICATION SYSTEMS

M. Tycz and M. W. Fitzmaurice

## INTRODUCTION

The rapidly increasing need for wideband communication systems for space-to-space and space-to-ground links in the late 1970's and early 1980's has stimulated an increased interest in optical communication technology. There are active NASA and DoD supported programs which are directed toward developing high data rate, nominally 300 MBps to 1 GBps, optical communication systems for space flight use. A typical system might employ a Nd:YAG mode-locked laser transmitter using on-off-key (OOK), binary polarization (BPM) or quaternary modulation formats and a photoemissive direct detection receiver incorporating either high speed, gated photomultiplier tubes or avalanche photodiode/low noise, wideband amplifier combinations. Such systems are governed by Poisson statistics [1-2]. Their performance for OOK or BPM modulation formats and deterministic average receiver signal intensity have previously been analyzed and reported in the literature [3-4].

Optical communication systems look most attractive in the space-to-space link. In this configuration, it is easiest to take full advantage of their relatively small size and weight, their rugged and long-lifetime components and their low prime power requirements. However, it is in this configuration, for example low-earth orbiter to synchronous satellite link, that the operational system may require sub-arcsecond pointing of the laser transmitter beam. As a result, a dominant noise source may be the interaction of the transmitter far field irradiance profile and the instantaneous transmitter pointing direction (see Figure 1). Thus, the average receiver signal level may be random and obey beta statistics [5-7]. For the space-to-ground link one can take advantage of the transmitter low power, light weight, etc. system parameters, but must contend with the perturbing effects of the atmosphere (see Figure 1). Performance analysis reported in the literature for the space-to-ground link incorporate the effects of atmospheric scintillation assuming a log-normal channel [8]. Although system performance analyses have not been completed for the Ricean and Rayleigh channels, theory does exist asserting that certain communication links will be subject to atmospheric scintillation resulting in time varying average signal amplitudes described by Ricean or Rayleigh probability distributions [9].

Coupling the advancement of the theoretical analyses of direct detection optical communication systems for varied channels with the rapidly progressing systems development, it now becomes necessary to design a laboratory device for controlled testing of the communication

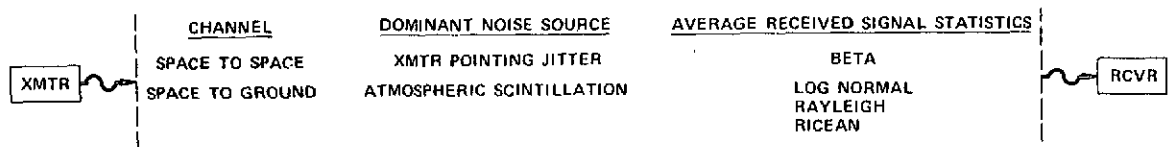


Figure 1. Direct detection optical communication channels

system. It is required that the unit simulate the channel effects of the different link configurations. This publication addresses the design and performance of one such Channel Simulator.

## CHANNEL SIMULATOR SYSTEM CONCEPT

The purpose of the Channel Simulator is to provide the controlled effects of atmospheric scintillation and transmitter pointing inaccuracy for testing and evaluating direct detection optical communication systems for the space-to-space and space-to-ground links. As seen in Figure 2a, the Channel Simulator transforms a constant signal  $I$  into a preselected random varying signal  $I_M$ . The probability distribution  $f_{I_M}(i_M)$  governing the modulated signal level of the Channel Simulator output  $I_M$  (see Figure 2b) will depend on the link to be simulated. The Channel Simulator described in this publication is designed to produce random signals whose time varying irradiance may obey log normal, chi-squared or beta statistics and whose time varying amplitude may obey log normal, Ricean or Rayleigh statistics. It consists of two major components: the linearized optical modulator and the processing electronics. Its transfer function is given by  $I_M = C V$  where  $I_M$  is the irradiance of the modulated light beam,  $C$  is a constant determined by the modulator crystal parameters and  $V$  is the voltage applied to the modulator. In general,  $V$  may be deterministic or random. If  $V$  is random with probability density  $f_V(v)$ , then the probability density governing  $I_M$  will be [10]

$$f_{I_M}(i_M) = \frac{f_V(i_M/C)}{|C|}. \quad (1)$$

## OPTICAL SUBSYSTEM

The optical subsystem consists either of a linearized acoustooptic modulator or a linearized electrooptic modulator. One such system utilized by the experimenters was a KDP electrooptic modulator. Employed in the transverse mode of operation, the modulation field was applied normal to the direction of light propagation. Using the axes defined in Figure 3, the input polarizer was in the  $X'Z$  plane at an angle of  $45^\circ$  from the  $Z$ -axis. The output polarizer was rotated  $90^\circ$  relative to the input. The transfer function for this modulator system is [11].

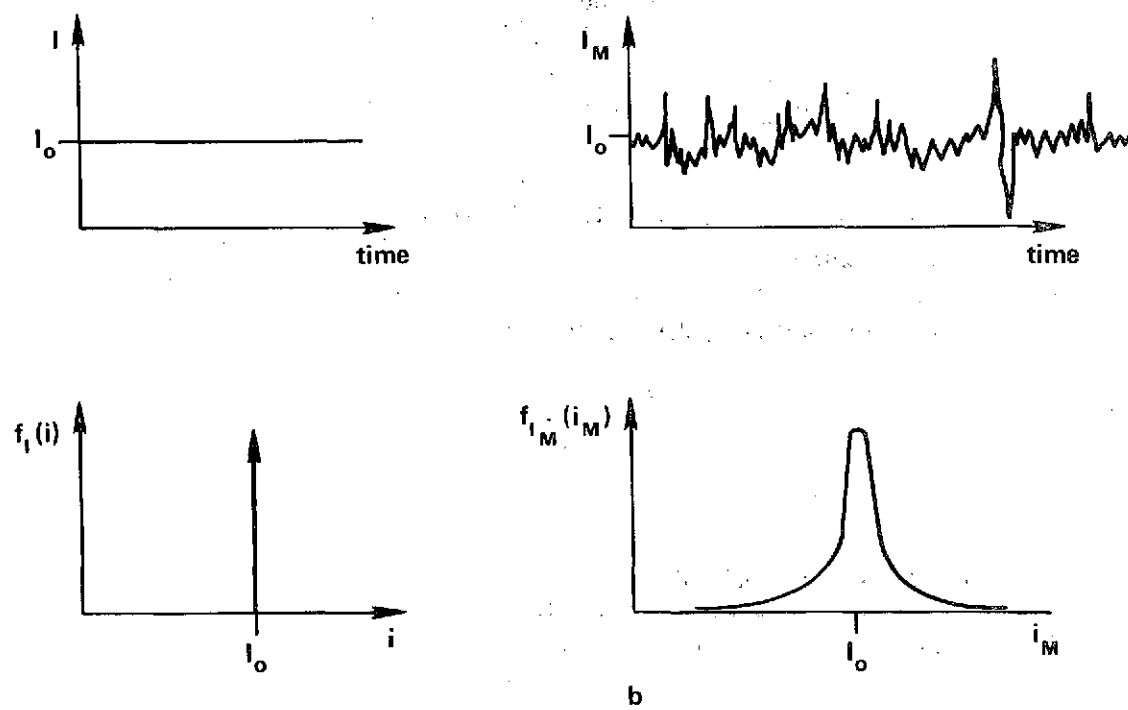
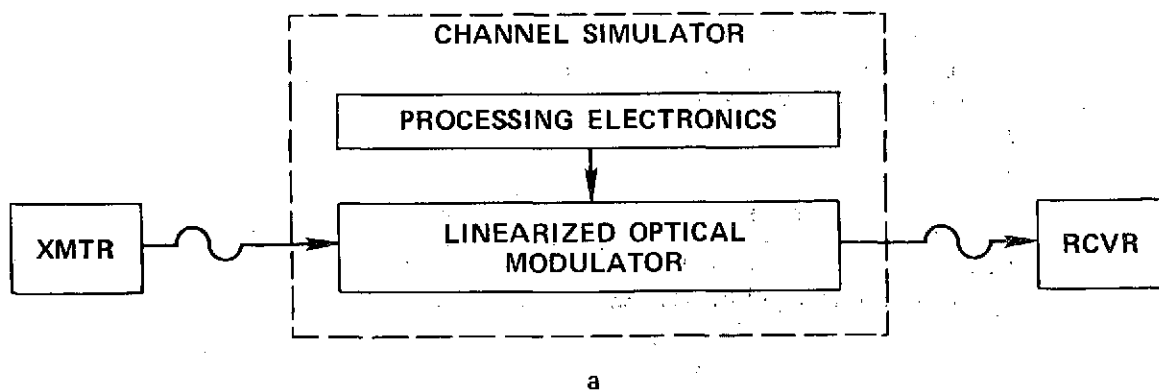


Figure 2. Channel simulator induced random signal perturbations.



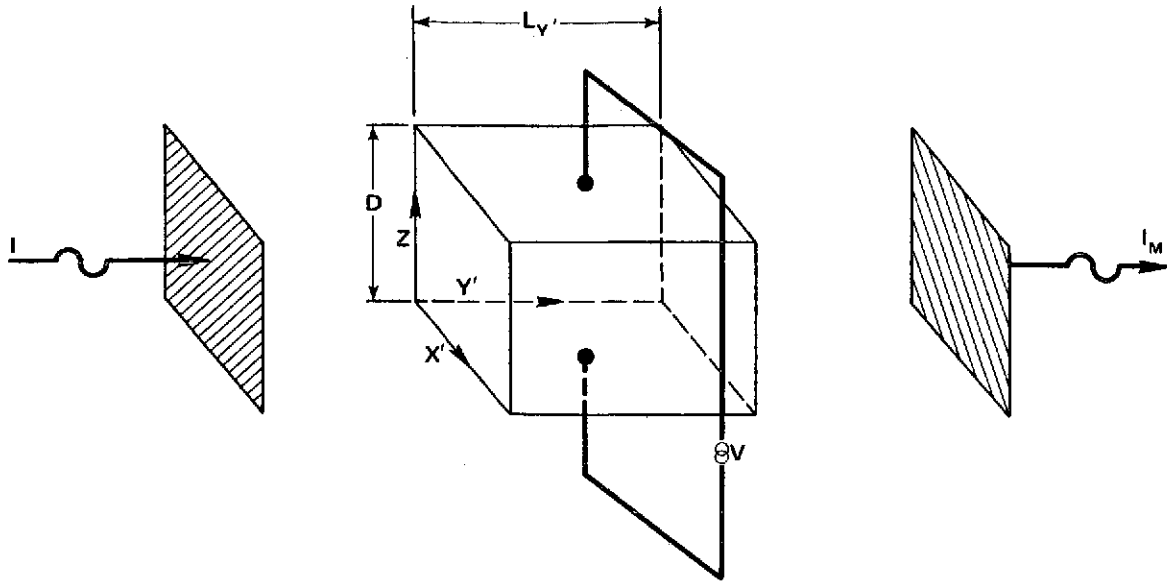


Figure 3. Electrooptic modulation – transverse mode.

$$\frac{I_{\text{TRANS}}}{I_{\text{INCID}}} = \sin^2 \frac{\omega}{2c} \left[ n_o \cdot n_e - \frac{n_o^3 r_{63} E_z}{2} \right] L_{y'} \equiv \sin^2 \frac{\Gamma}{2} \quad (2)$$

where  $\omega$  is the frequency of incident light,  $c$  is the speed of light,  $n_o$  and  $n_e$  are the ordinary and extraordinary indices of refraction,  $E_z$  is the applied field,  $r_{63}$  is the electrooptic coefficient of the KDP crystal and  $(n_o \cdot n_e) L_{y'} \omega/2c$ , the retardation due to natural birefringence, is a function of temperature and can be compensated. Therefore, consider

$$\frac{\Gamma^*}{2} = - \frac{\omega n_o^3}{4c} r_{63} E_z L_{y'}. \quad (3)$$

If we define  $E_z = V/D$  and let

$$V_{1/2} = - \frac{4cD}{\omega n_o^3 r_{63} L_{y'}} \frac{\pi}{2} \quad (4)$$

then

$$\frac{I_{\text{TRANS}}}{I_{\text{INCID}}} = \sin^2 \frac{\Gamma^*}{2} = \sin^2 \frac{\pi V}{2 V_{1/2}} \quad (5)$$

where  $V_{1/2}$  is the voltage required from maximum transmission through the crystal.

If we perform a series expansion of the right hand side of equation 5, then

$$\frac{I_{\text{TRANS}}}{I_{\text{INCID}}} = \left[ \frac{\pi V}{2V_{1/2}} - \left( \frac{\pi V}{2V_{1/2}} \right)^3 \frac{1}{3!} + \left( \frac{\pi V}{2V_{1/2}} \right)^5 \frac{1}{5!} - \left( \frac{\pi V}{2V_{1/2}} \right)^7 \frac{1}{7!} + \dots \right]^2 \quad (6)$$

It is obvious that for  $V \ll V_{1/2}$

$$\frac{I_{\text{TRANS}}}{I_{\text{INCID}}} = \frac{\pi^2 V^2}{4 V_{1/2}^2} \quad (7)$$

One can now form a linearized optical modulator system by simply inserting a square root module between the applied voltage  $V$  and the modulator crystal, assuming operation in the range  $V \ll V_{1/2}$ .

The linearized acoustooptic modulator is designed using the same principal. Modulation of light due to the interaction of a light wave with a sound wave induces a diffracted light wave at the sum or difference frequency. The transfer function for a beam incident into a medium of a distance  $\ell$  is given by [12]

$$\frac{I_{\text{DIFF}}}{I_{\text{INCID}}} = \sin^2 \left[ \frac{\pi \ell \sqrt{2}}{2 \lambda_0} \sqrt{I_{\text{ACOUSTIC}} \frac{n^6 p^2}{\rho v_s^3}} \right] \quad (8)$$

where  $\lambda_0$  is the wavelength of the incident wave in a vacuum,  $p$  is the photoelastic constant of the medium,  $I_{\text{ACOUSTIC}}$  the acoustic intensity,  $v_s$  is the velocity of sound in the acoustic medium and  $\rho$  the mass density. Defining  $I_0$  as a reference acoustic intensity yielding maximum deflection

$$\sqrt{I_0} = \frac{\lambda_0}{\sqrt{2} \ell} \sqrt{\frac{\rho v_s^3}{n^6 p^2}} \quad (9)$$

and noting that  $\sqrt{I}$  is proportional to  $V$  the applied voltage, then

$$\frac{I_{\text{DIFF}}}{I_{\text{INCID}}} = \sin^2 \frac{\pi V}{2 V_0} \quad (10)$$

Using the same expansion as before and assuming voltages  $V \ll V_0$ , then the transfer function becomes linear where once again a square rooting device is inserted before the modulator crystal

$$I_{\text{DIFF}} = I_{\text{INCID}} \frac{\pi^2 (\sqrt{V})^2}{4 V_0^2} = C V. \quad (11)$$

Results of this technique applied to the Channel Simulator will be presented later in this publication.

## PROCESSING ELECTRONICS

The analog processing electronics generate the random voltages necessary to drive the optical modulator for simulating the desired channels. As seen in Figure 4a, it consists of Gaussian random signal generators fed into antilog converters, squaring modules and similar devices which perform appropriate mathematical operations. Although certain operations are shared by more than one channel, the transfer function for each channel will be presented separately for clarity.

### Atmospheric Log Normal Channel

For the atmospheric scintillation channel log normal mode, the random variable that obeys log normal statistics is  $I/I_0$  or the instantaneous irradiance divided by the mean irradiance. To simulate the log normal behavior of this channel the following random variable  $I_M$  need be generated:

$$I_M = I_0 e^{2L} \quad (12)$$

where  $2L$  is Gaussian with mean  $K$  and variance  $\lambda^2$  [13]. The transfer function of the channel simulator log normal channel (see Figure 4b) from the Gaussian input, monitored at test point TP7, to the modulated irradiance output is given by

$$I_M = \frac{bC}{10} e^{-2(X_{\text{TP7}} + A) \ln 10/10} \quad (13)$$

where  $A$  is the log normal offset,  $b$  is the gain established by the last amplifier stage,  $X_{\text{TP7}}$  is a zero mean Gaussian random voltage with variance  $\sigma_{X_{\text{TP7}}}^2$ , and  $C$  is the linearized modulator subsystem constant of proportionality.

Redefining variables in equation 13 results in equation 12 where  $I_0 \equiv bC/10$  and  $L \equiv -(X_{\text{TP7}} + A) \ln 10/10$ . Additionally, when simulating the log normal channel, the log

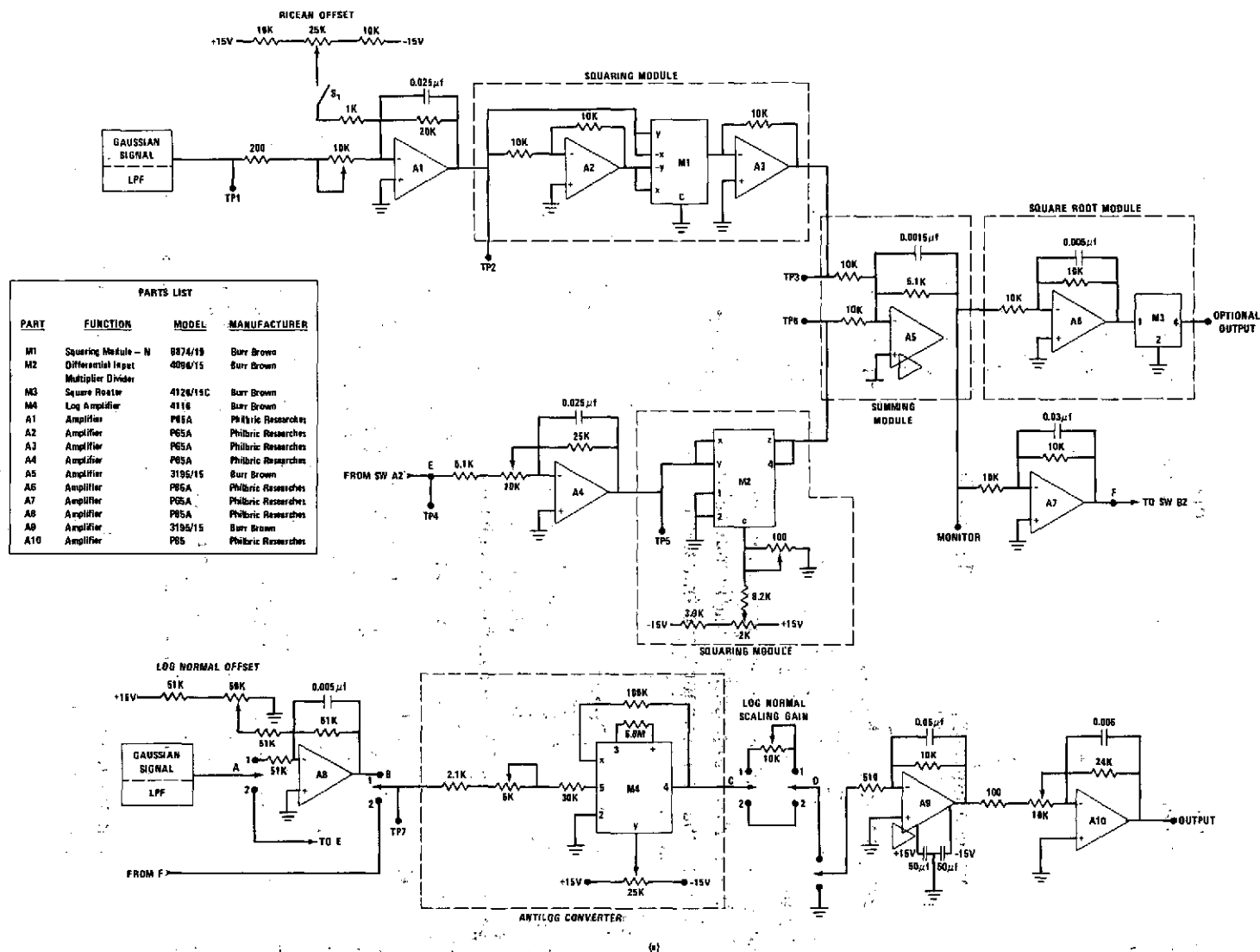
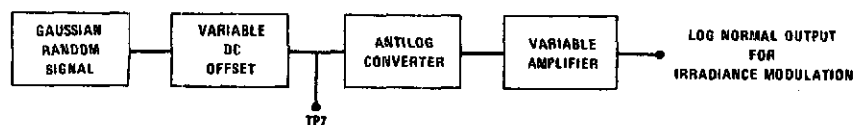
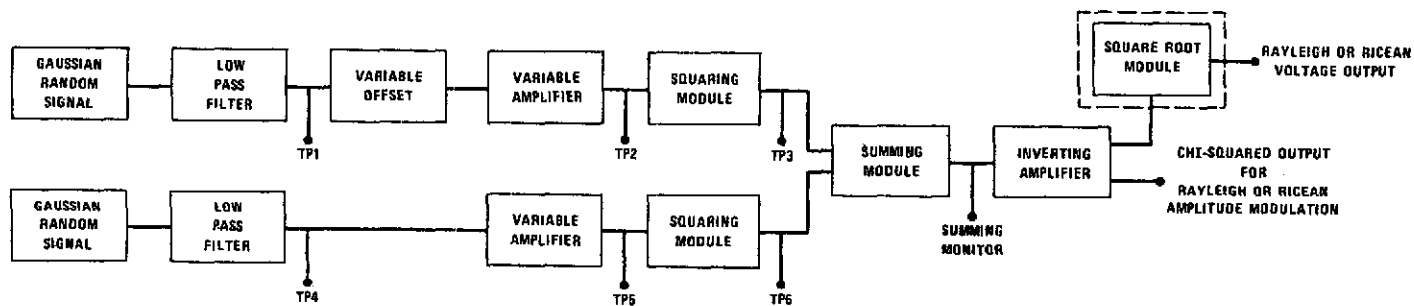


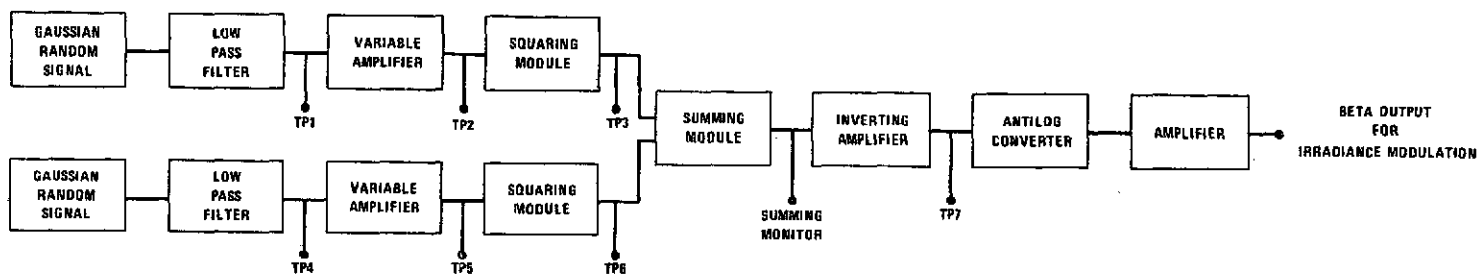
Figure 4. Channel simulator processing electronics (a) composite of all channels (b) log normal atmospheric channel (c) Raleigh or Ricean atmospheric channel (d) beta free space channel.



(b)



(c)



(d)

Figure 4 (continued)

amplitude must have a mean equal to negative of its variance  $s^2$  [14]. Therefore, letting  $E\{L\} = -\text{Var}\{L\} = -s^2$  we establish relationships for the values of A and  $\sigma_{X_{TP7}}^2$  with  $s^2$ :

$$A = s^2 10/\ln 10 \quad (14)$$

$$\sigma_{X_{TP7}}^2 = s^2 [10/\ln 10]^2. \quad (15)$$

The value of  $s^2$  is selected from atmospheric scintillation data and ranges nominally from  $s^2 = 0.01$  to  $s^2 = 0.1$  [15].

### Atmospheric Rayleigh and Ricean Channel

For the atmospheric scintillation channel Rayleigh or Ricean mode, the random variable that is described by these statistics is the light amplitude. Until now, however, the linear transfer function of the Channel Simulator has been referenced to the irradiance level of the output. The light amplitude transfer function is thus

$$A = [C V]^{1/2} = C_a V^{1/2} \quad (16)$$

where  $C_a = C^{1/2}$ .

A Rayleigh or Ricean random variable P can be generated by the following

$$P = [X_1^2 + X_2^2]^{1/2} \quad (17)$$

where for the Ricean case  $X_1$  and  $X_2$  are independent Gaussian random variables with means  $\mu_1$  and  $\mu_2$  and variances  $\sigma_1^2 = \sigma_2^2$ . For the Rayleigh case,  $\mu_1 = \mu_2 = 0$  [16].

The total transfer function of the Ricean\* channel from the Gaussian inputs to the modulated light amplitude output is given by (see Figure 4c)

$$P = \left[ C \left\{ \frac{(X_{TP2} + d)^2}{20} + \frac{X_{TP5}^2}{20} \right\} \right]^{1/2} = C_a V^{1/2} \quad (18)$$

where  $X_{TP2}$  and  $X_{TP5}$  are zero mean independent Gaussian random variables with variance  $\sigma^2$ , and d is the Ricean offset. Note also that for Rayleigh simulation V and therefore the modulated irradiance is a chi-squared random variable with two degrees of freedom.

---

\*Since it is more general, we present this channel with the understanding that for the Rayleigh case the offset is simply set to zero.

### Free Space Channel

For satellite to satellite optical communications, signal fades caused by pointing jitter may limit receiver performance. In this case, the modulation on the average received signal level will be described by beta statistics [5-7]. In simulating this fading condition the following must be satisfied:

$$I_M = I_0 e^{-\rho^2/2\xi^2} \quad (19)$$

where  $I_0$  corresponds to the peak of the spatial Gaussian irradiance profile,  $\xi$  is the transmitter beam half angle at the  $1/e^2$  points and  $\rho$  is the distance the beam is from the center of the receiving aperture. For typical systems,  $\rho^2$  is a chi-squared random variable of two degrees of freedom corresponding to two independent and orthogonal Gaussian tracking error signals.

The total transfer function of the Channel Simulator in the beta mode of operation can be seen in Figure 4d. From the Gaussian random voltage inputs to the modulated irradiance output the relationship is

$$I_M = 10C e^{-(\ln 10/5)[(X_{TP2}^2 + X_{TP5}^2)/20]} \quad (20)$$

where  $X_{TP2}$  and  $X_{TP5}$  are zero mean, equal variance, Gaussian random variables. Redefining

$$\begin{aligned} I_0 &= 10C \\ \sigma^2 &= \text{Var}\{X_{TP2}\} = \text{Var}\{X_{TP5}\} \\ \xi^2 &= 50/\ln 10 \end{aligned} \quad (21)$$

and

$$\rho^2 = X_{TP2}^2 + X_{TP5}^2,$$

then equation 19 is satisfied and the density of  $I_M$  becomes

$$f_{I_M}(i_M) = \frac{\xi^2}{\sigma^2} \left( \frac{1}{I_0} \right)^{\xi^2/\sigma^2} (i_M)^{\xi^2/\sigma^2 - 1} \quad 0 \leq i_M \leq I_0. \quad (22)$$

The ratio of  $\xi/\sigma$  is determined by both system design and the link to be considered and will vary typically from 3 to 10 [7].

### COMPONENT TRANSFER FUNCTION TEST RESULTS

Tests have been performed on the Channel Simulator processing electronics and optical modulator subsystem to verify the accuracy of the mathematical operations, the linearity of

the optical modulator and the independence of the Gaussian sources. Figure 5 shows the results of tests performed on the electronic modules which perform the required mathematical operation within the processing electronics. The equations representing the resultant curves were derived from the data assuming minimum mean square error fit to a straight line, least square fit to a power curve and least squares fit to an exponential curve where appropriate.

The transfer function of the linearized acoustooptic modulator system used by the authors was tested using a helium-neon laser input beam and an S-20 photomultiplier detector. Figure 6 shows typical test results when the modulator bias and the photomultiplier tube voltage are set for linear operation. Since the slope of this transfer function is directly affected by the photomultiplier tube gain as well as the modulation index, this test was performed before each of the channel simulations.

As previously stated, operation of the Channel Simulator for the beta, Rayleigh and Ricean modes assumes that the Gaussian random voltage inputs at test points TP2 and TP5 are zero-mean, equal variance and independent. Offset adjustments as well as variable gain stages are provided to ensure that the signals are zero mean and equal variance. Tests for independence were performed using the Hewlett Packard Correlator, Model 3729A. Recall that two random signals X and Y are independent if their crosscorrelation coefficient  $\rho_{XY}$  is zero, i.e.,

$$\rho = \frac{E\{XY\} - E\{X\} E\{Y\}}{\sqrt{\text{Var}\{X\} \text{Var}\{Y\}}} = 0 \quad (23)$$

where for this case, the means  $E\{X\}$  and  $E\{Y\}$  are zero and the  $\text{VAR}\{X\} = \text{VAR}\{Y\}$  is simply the autocorrelation of X or Y evaluated at a time delay of zero, and  $E\{XY\}$  is the crosscorrelation evaluated at a time delay of zero. The auto and crosscorrelation of  $X_{TP2}$  and  $X_{TP5}$  were taken for Ricean offset  $d = 0$ . Using these values at delay zero and substituting into equation 23 resulted with the crosscorrelation coefficient  $\rho = 0.006$ .

## STATISTICAL FUNCTION TEST RESULTS

The usefulness of the Channel Simulator is measured in terms of its ability to accurately simulate the desired channel. Figure 7 demonstrates the performance of the log normal channel simulation as compared to experimentally measured channel perturbations. The plot of log amplitude versus its cumulative probability is on a log normal cumulative probability graph. The solid line represents typical results from a GEOS B satellite experiment [15] for which an argon laser beacon was transmitted through the atmosphere to a low earth orbiting satellite. The instantaneous signal was detected on-board the spacecraft by a photomultiplier tube and was telemetried to ground for statistical analyses. The dashed lines represent data taken from the Channel Simulator system in which the signal



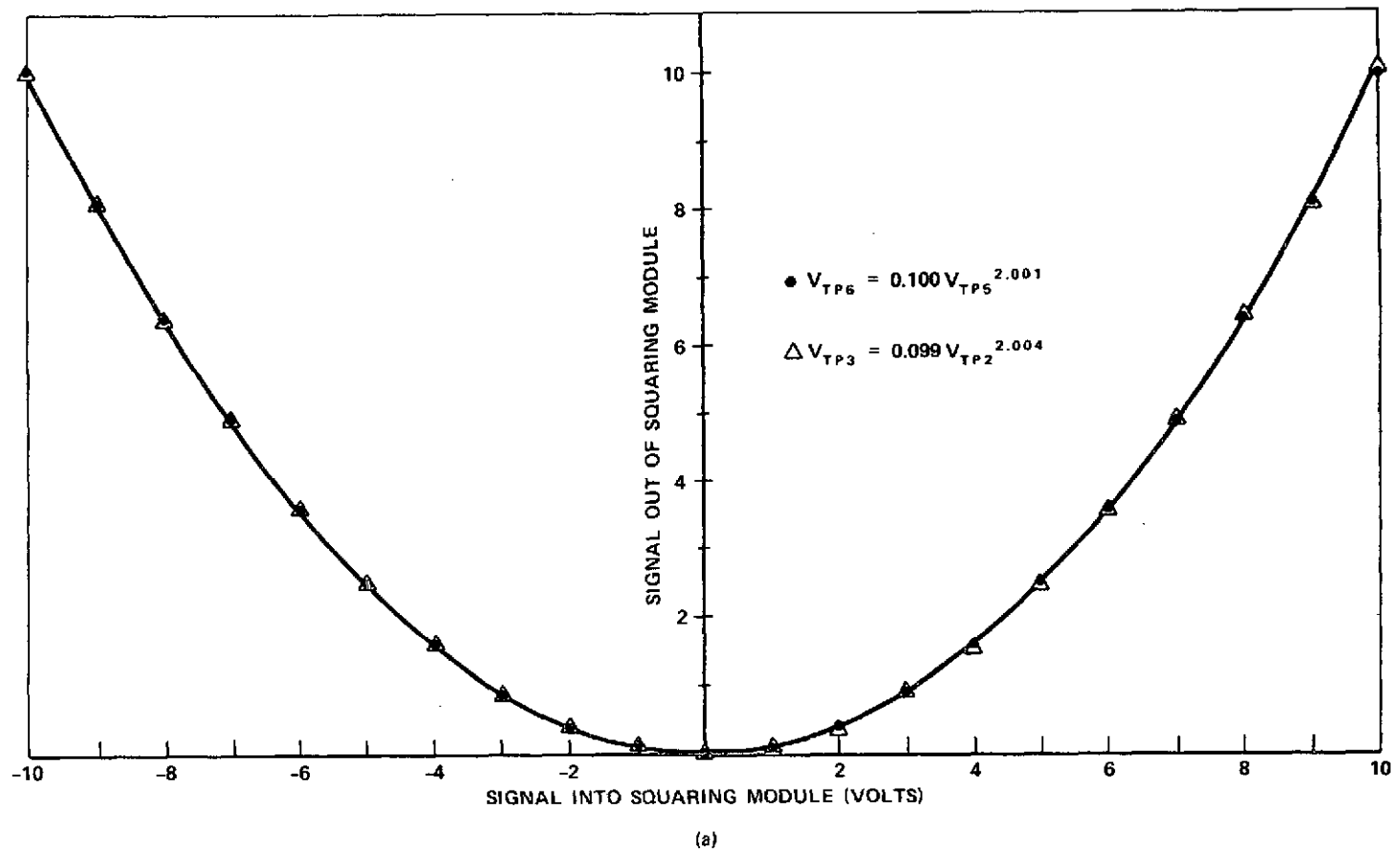
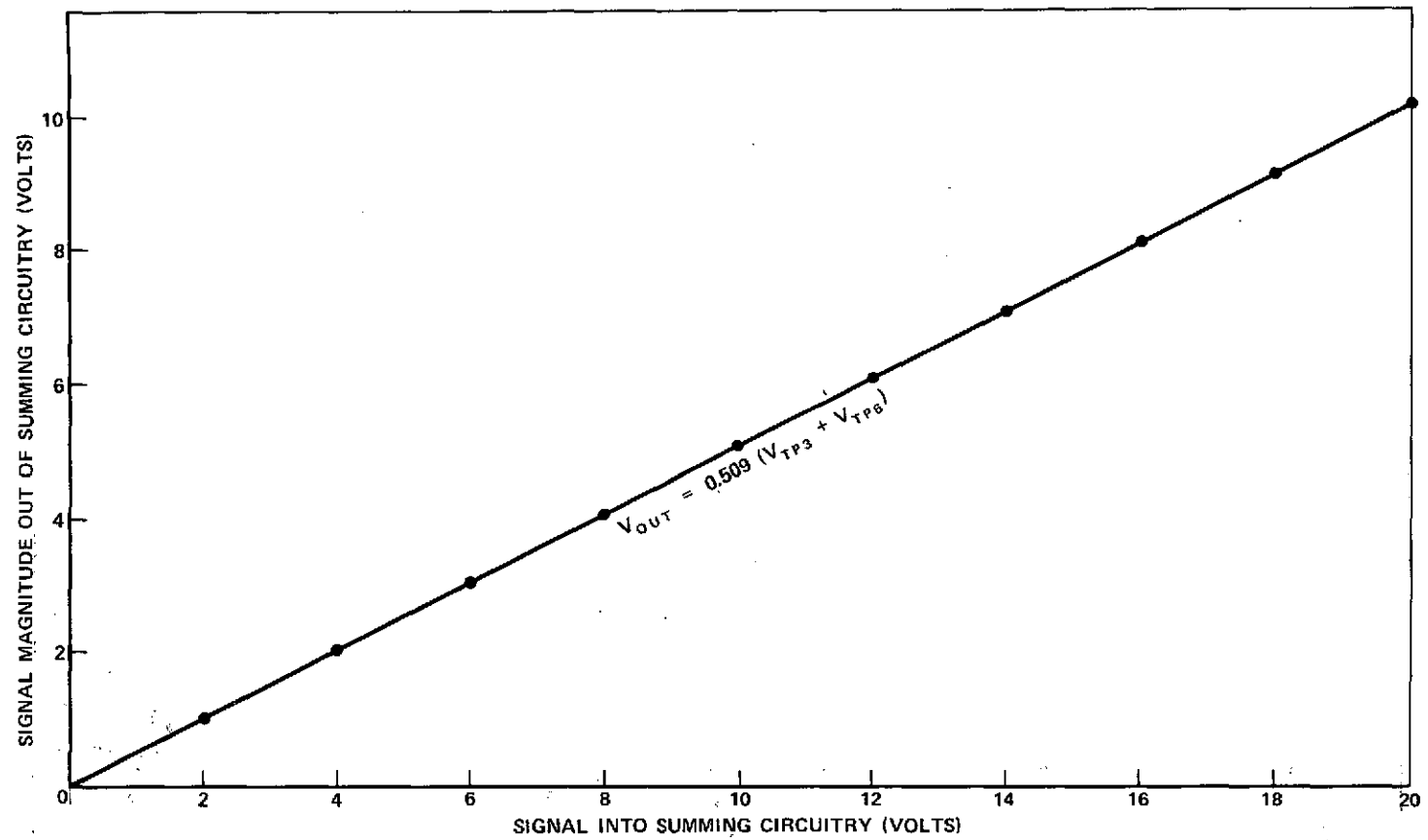


Figure 5. Transfer functions of mathematical operations.



(b)

Figure 5 (continued)

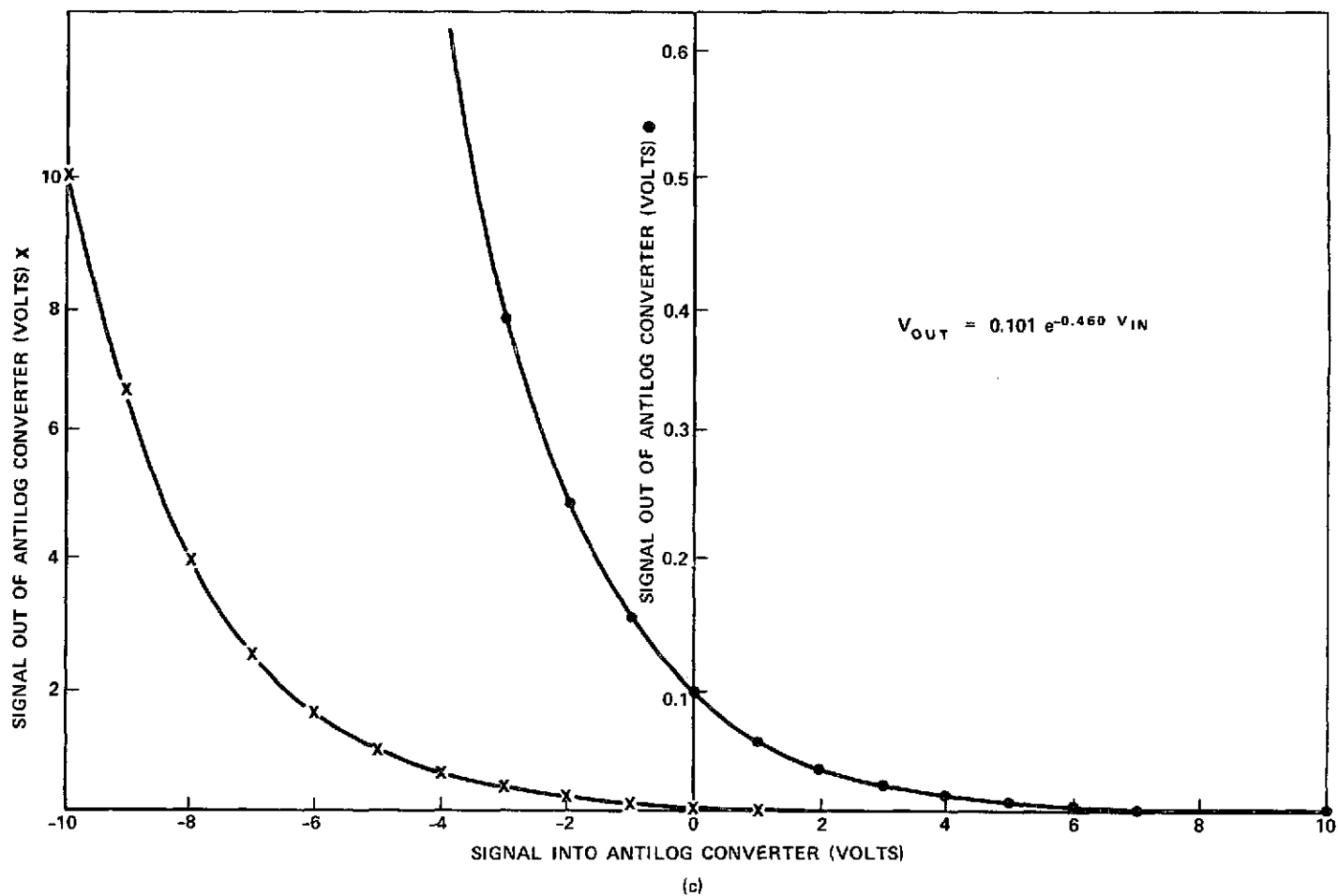


Figure 5 (continued)

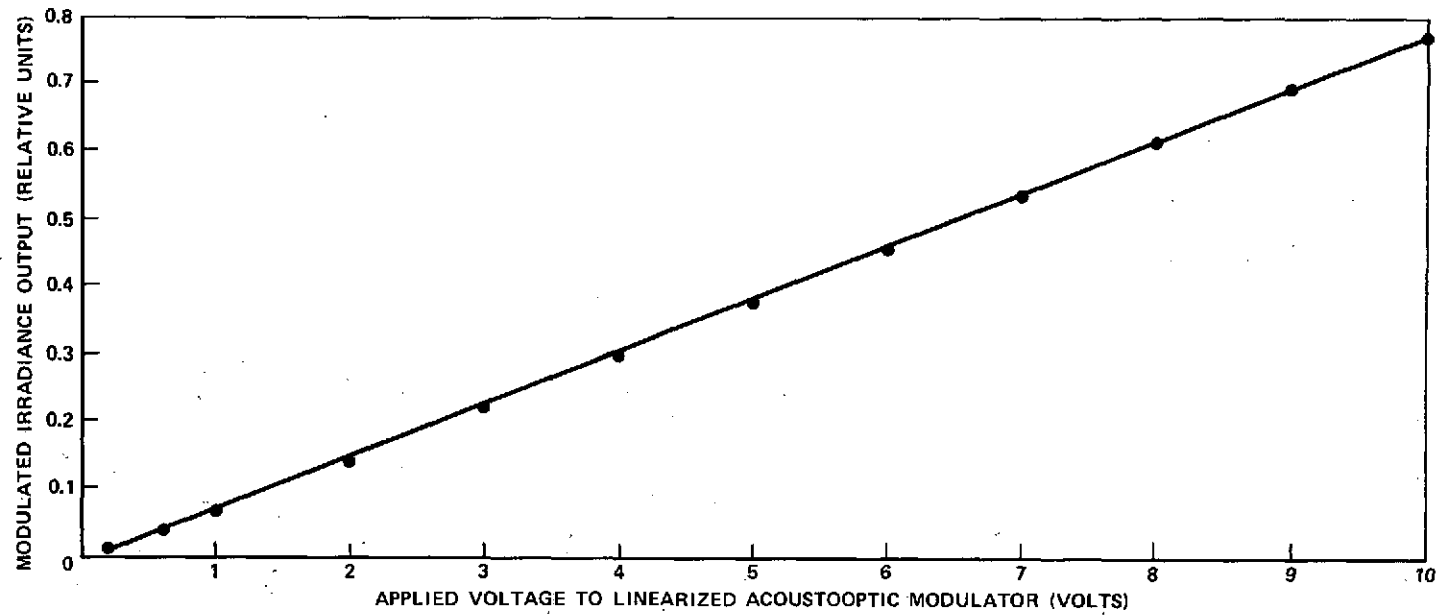


Figure 6. Transfer function of the linearized acoustooptic modulator.

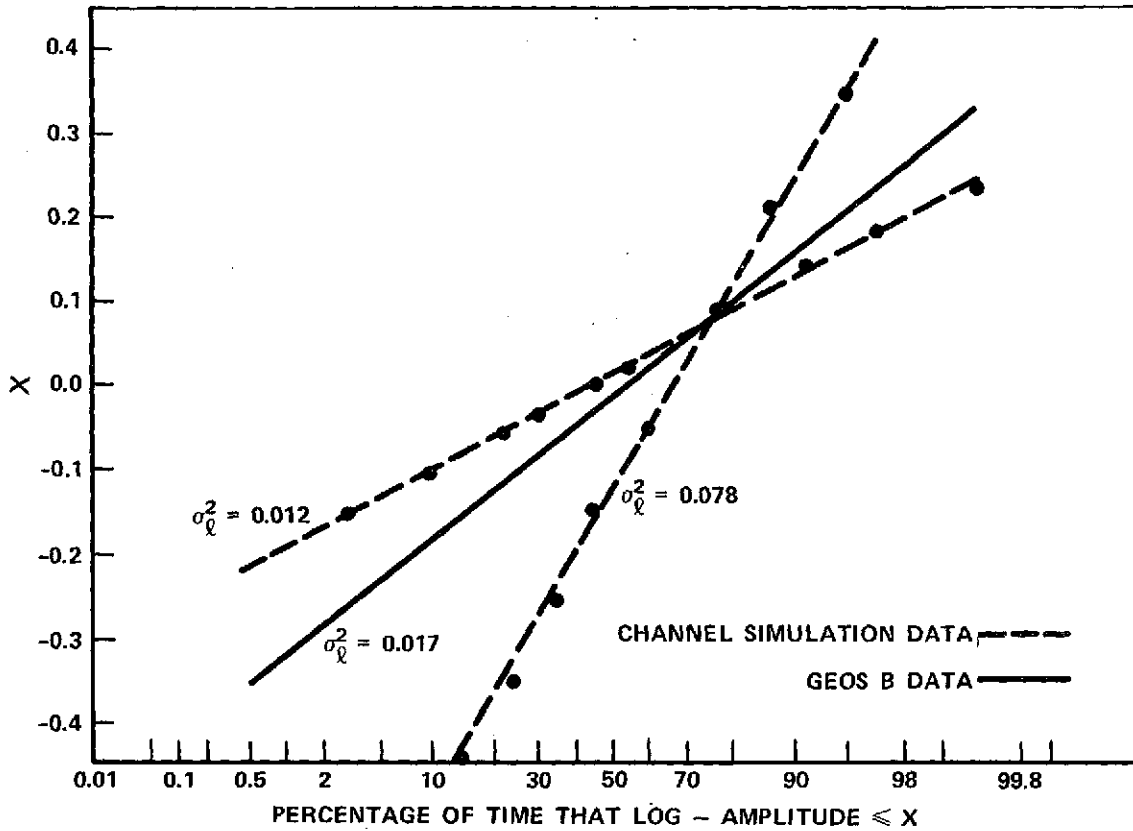


Figure 7. Comparison of channel simulator log-normal statistics with GEOS-B data.

level was log normally modulated. The linearity of the data indicates the modulated signal is indeed log normally distributed and the slope specifies the strength of atmospheric scintillation. The latter can be made to vary from a log amplitude variance of 0.01 to 0.08.

Performance of the beta channel requires operation of all the mathematical functions in the processing electronics. The output signal of the Rayleigh and Ricean channel is the input signal provided to the antilog converter for generating a beta distributed random variable. Thus accurate simulation of the beta distribution necessitates good performance of the Ricean and Rayleigh atmospheric channel modes.

Recall that the probability density function governing the beta mode of operation was given by equation 22. Therefore, the cumulative density will satisfy

$$F_{I_M}(i_M) = \int_0^{i_M} \frac{\xi^2}{\sigma^2} I_0^{-\xi^2/\sigma^2} i^{\xi^2/\sigma^2 - 1} di = \left( \frac{1}{I_0} \right)^{\xi^2/\sigma^2} i_M^{\xi^2/\sigma^2}. \quad (24)$$

Taking logarithm of both sides gives

$$\log F_{I_M}(i_M) = \frac{\xi^2}{\sigma^2} \log i_M - \frac{\xi^2}{\sigma^2} \log I_0. \quad (25)$$

Plotting the logarithm of the cumulative beta density versus the logarithm of the relative modulated signal level irradiance results in a linear curve, the slope of which is the parameter of the beta distribution to be simulated. Figure 8 shows a typical plot of simulated beta modulation for which the ratio  $\xi/\sigma = 5.3$ . The Channel Simulator can be made to simulate the space-to-space link with beta perturbations ranging nominally from  $1 \leq \xi/\sigma \leq 10$ .

Although not directly applicable to simulating optical communication channel effects, an additional mode of operation has been coupled to the system. By adding an optional square rooting stage to the output of the Rayleigh and Ricean channel, the voltage output and, therefore, the modulated irradiance (as opposed to the modulated E-field) becomes Rayleigh or Ricean distributed. A test was performed on the operation of this Rayleigh random voltage output. Recall that a Rayleigh distributed random variable  $P$  has cumulative density

$$F_P(\rho) = \frac{1}{2\pi\sigma^2} \int_0^\rho 2\pi r e^{-r^2/2\sigma^2} dr, \quad \rho \geq 0 \quad (26)$$

where  $\sigma^2$  is the parameter of the Rayleigh distribution. Performing the integration in equation 26 results with

$$\sqrt{-\ln[1 - F(\rho)]} = \frac{1}{\sqrt{2\sigma^2}} \rho. \quad (27)$$

Figure 9 is a plot of equation 27 using the square root output voltage for data. The linearity of the data indicates that the voltage is Rayleigh distributed and the slope indicates the value of the Rayleigh parameter,  $\sigma^2 = 10.3 \text{ V}^2$ .

## CONCLUSIONS

The system discussed in the previous sections for simulating the effects of space-to-space and space-to-ground optical communication channels is relatively easy to construct and enables controlled tests to be performed in the laboratory. The ultimate utility of the simulator is dependent on the validity of the theoretical models chosen to represent each channel. When coupled with a laser source, the Channel Simulator is capable of providing log normal, Rayleigh, Ricean, chi-squared or beta irradiance modulation and voltages as well as Rayleigh and Ricean modulated electric fields. It is intended that the simulator discussed in this paper will be incorporated into a high data rate optical communication system for laboratory testing of

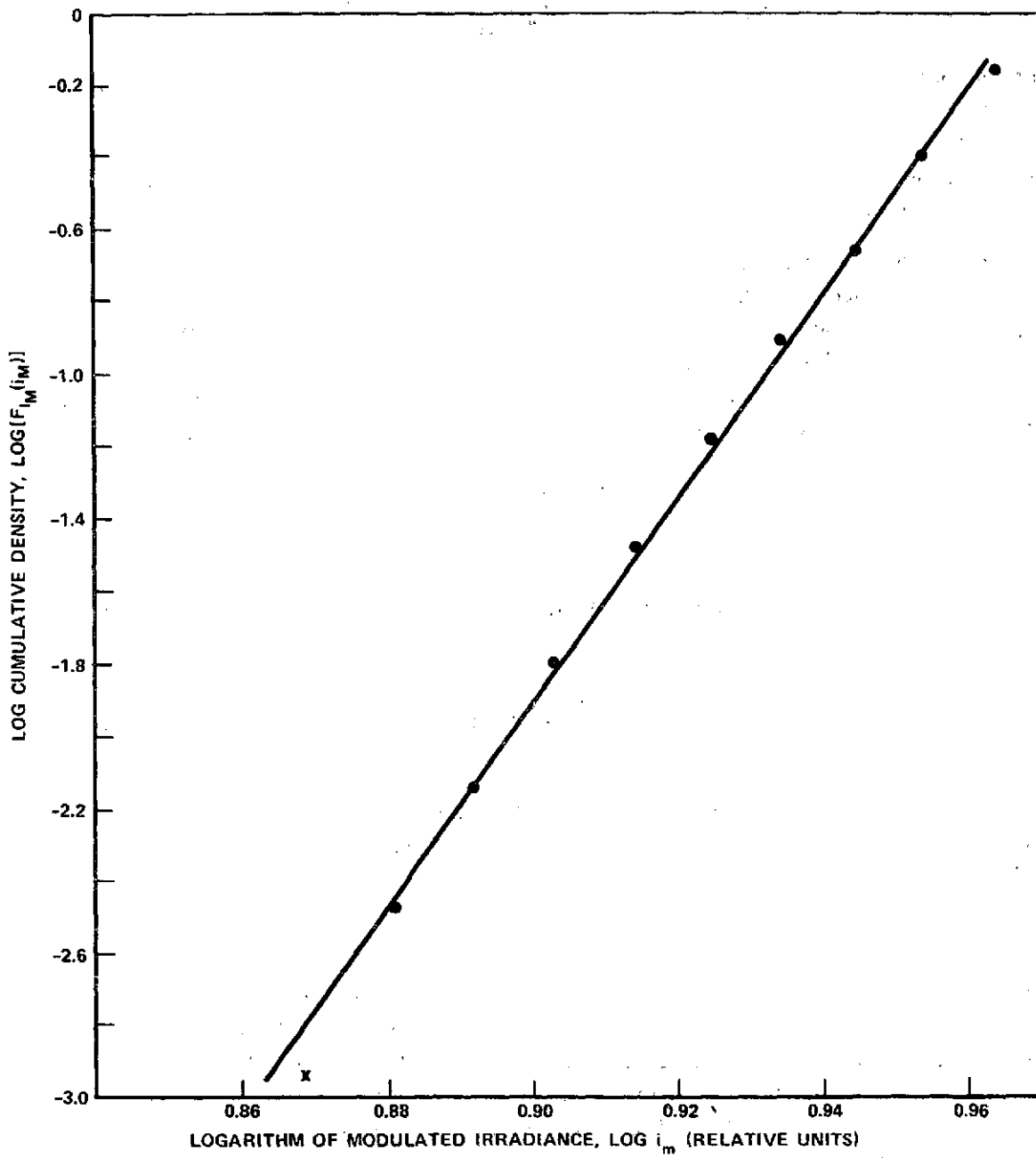


Figure 8. Statistical test of beta channel.

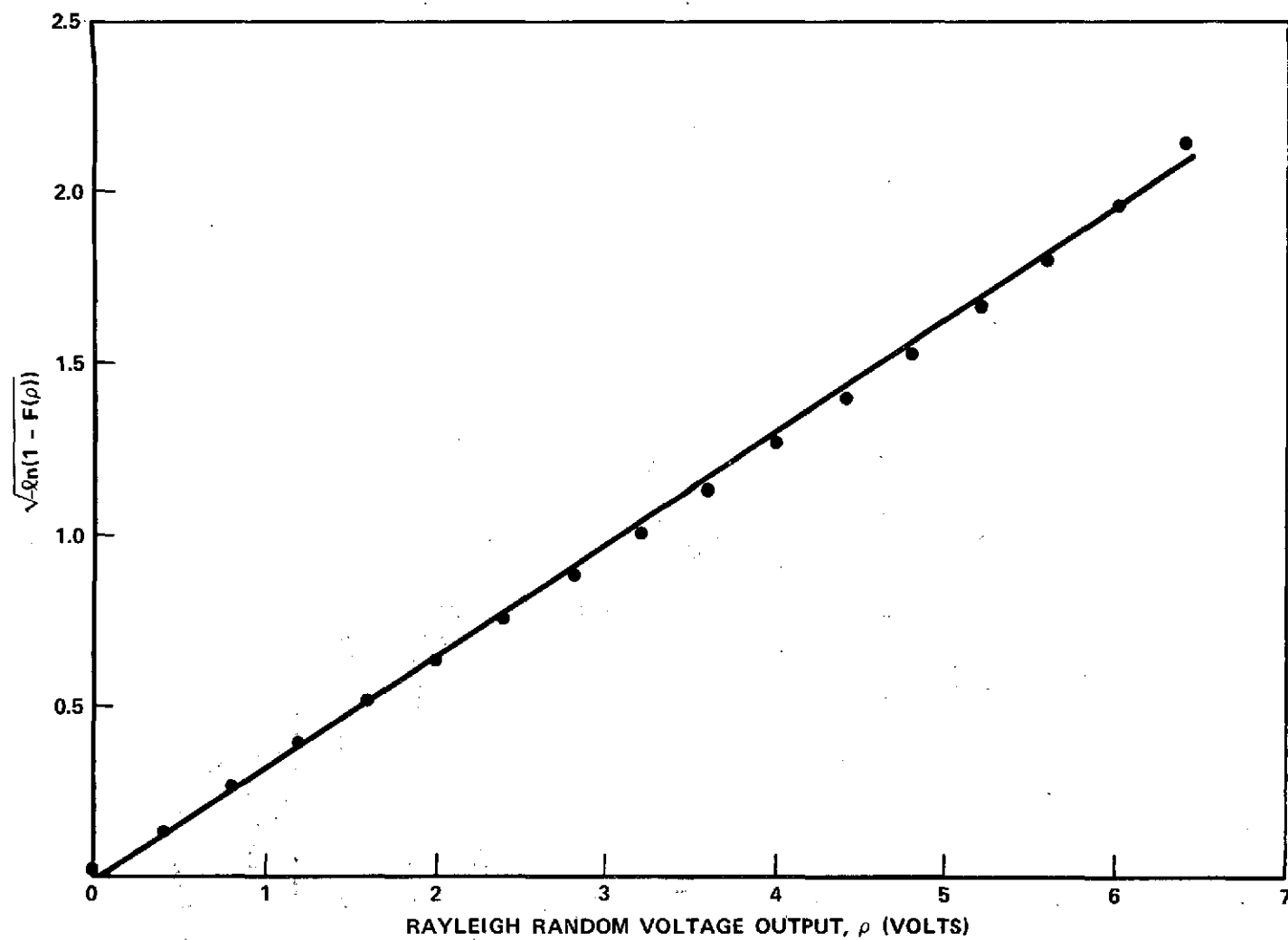


Figure 9. Statistical test of Rayleigh random voltage mode of operation.



the composite system performance. Comparisons with computer generated analyses will then be made to evaluate the accuracy of current analytical models for laser communication links undergoing fading.

## ACKNOWLEDGMENTS

The authors thank Jim Abshire and Dave Zackowski for technical assistance in the construction and testing of components.

## REFERENCES

- [1] R. J. Glauber, "Optical Coherence and Photon Statistics," in Quantum Optics and Electronics, C. de Witt et al., Ed. New York: Gordon and Breach, 1965, pp. 65-185.
- [2] L. Mandel and E. Wolf, "Coherence Properties of Optical Fields," Rev. Mod. Phys., Vol. 37, pp. 231-287, Apr. 1965.
- [3] T. F. Curran and M. Ross, "Optimum Detection Thresholds in Optical Communications," Proc. IEEE, Vol. 53, pp. 1770-1771, Nov. 1965.
- [4] W. K. Pratt, Laser Communication Systems, New York, Wiley, 1969, pp. 171-173, 208-210.
- [5] P. Titterton, "Power Reduction and Fluctuation Caused by Narrow Laser Beam Motion in the Far Field," Appl. Opt., Vol. 12, pp. 423-425, Feb. 1973.
- [6] D. L. Fried, "Statistics of Laser Beam Fade Induced by Pointing Jitter," Appl. Opt., Vol. 12, pp. 422-423, Feb. 1973.
- [7] M. Tycz, M. Fitzmaurice and D. Premo, "Optical Communication System Performance with Tracking Error Induced Signal Fading," IEEE Trans. on Comm., Vol. Com-21, No. 9, pp. 1069-1072, Sept. 1973.
- [8] P. Titterton and J. P. Speck, "Probability of Bit Error for an Optical Binary Communication Link in the Presence of Atmospheric Scintillation: Poisson Case," Appl. Opt., Vol. 12, pp. 425-426, Feb. 1973.
- [9] D. A. de Wolf, "Are Strong Irradiance Fluctuations Log Normal or Rayleigh Distributed?" J. Opt. Soc. Am., Vol. 59, pp. 1455-1460, Nov. 1969.

- [10] A. Papoulis, Probability, Random Variables and Stochastic Processes, New York, McGraw Hill, 1965, p. 127.
- [11] A. Yariv, Quantum Electronics, New York, Wiley, 1968, pp. 310-315.
- [12] A. Yariv, Introduction to Optical Electronics, New York, Holt, Rinehart and Winston, 1971, pp. 305-317.
- [13] E. Kreyszig, Introductory Mathematical Statistics, New York, Wiley, 1970, p. 114.
- [14] D. L. Fried, "Aperture Averaging of Scintillation," J. Opt. Soc. Am., Vol. 57, pp. 169-175, Feb. 1967.
- [15] P. Minott, "Scintillation in an Earth-to-Space Propagation Path," J. Opt. Soc. Am., Vol. 62, No. 7, pp. 885-888, July 1972.
- [16] J. Papoulis, Op. Cit., pp. 195-196.